RESEARCH ARTICLE | MARCH 23 2018

The role of Herzberg-Teller effects on the resonance Raman spectrum of *trans*-porphycene investigated by time dependent density functional theory

Julien Guthmuller

J. Chem. Phys. 148, 124107 (2018)
https://doi.org/10.1063/1.5023653

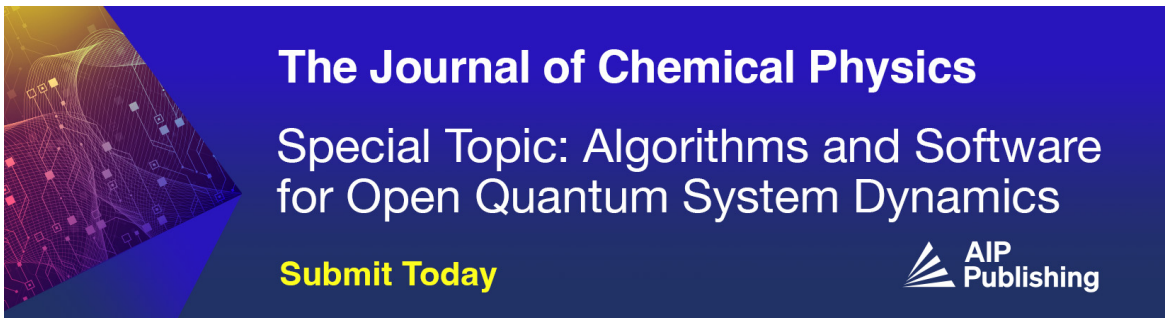

The role of Herzberg-Teller effects on the resonance Raman spectrum of *trans*-porphycene investigated by time dependent density functional theory

Julien Guthmuller
Faculty of Applied Physics and Mathematics, Gdańsk University of Technology, Narutowicza 11/12, 80-233 Gdańsk, Poland

(Received 26 January 2018; accepted 9 March 2018; published online 23 March 2018)

The S_1 excited state properties as well as the associated absorption and resonance Raman (RR) spectra of *trans*-porphycene are investigated by means of time dependent density functional theory calculations. The relative magnitude of the Franck-Condon (FC) contribution and of the Herzberg-Teller (HT) effects is evaluated for both the absorption and RR intensities. The accuracy of the calculated spectra is assessed by employing different theoretical approximations and by comparing with experimental data. The obtained results show that Duschinsky effects lead to noticeable modifications in the absorption intensities but are nearly negligible in the RR spectrum. By contrast, the HT effects are stronger for the RR intensities compared to the absorption intensities, and these effects significantly improve the agreement with the experimental RR spectrum. Moreover, the HT effects produce different values of the RR depolarization ratios, which can be used to quantify the relative importance of the FC and HT contributions. Generally, it is found that the HT effects have a significant role on the RR spectrum of *trans*-porphycene and that their inclusion in the computational scheme is mandatory to accurately predict the RR intensities. *Published by AIP Publishing.* https://doi.org/10.1063/1.5023653

I. INTRODUCTION

The spectroscopy of resonance Raman (RR) scattering is a widely used technique, which has proven to be an excellent tool for studying the dynamics and structure of molecular excited states.[1–3] Indeed, the RR intensities, which are associated with the ground state vibrational frequencies, carry specific information about the electronic excited states in resonance. In particular, the enhancement of the RR intensities is directly connected to the geometrical modifications between the ground state and the excited state[4–8] (i.e., displacements). Moreover, the RR intensities are also determined by the changes of vibrational frequencies and of vibrational modes going from the ground to the excited state[9] (i.e., Duschinsky rotation), by the vibronic structure arising from the Franck-Condon (FC) factors[10,11] as well as by the relative magnitudes of the electronic transition dipole moments[12,13] and of their derivatives. To investigate the influence of these parameters, different computational methodologies were proposed in the literature, which can be classified into two families. The first type of method is based on an explicit evaluation of the sum-over-state expression for the Raman polarizability tensor (see, e.g., Refs. 14–17), while the second type of method corresponds to a time dependent approach, which is based on wave packet dynamics (see, e.g., Refs. 18–23). Within this framework, several studies have focused recently on the inclusion of Herzberg-Teller (HT) effects[17,22–25] both for the calculation of RR spectra and for the related spectroscopy of absorption. While the FC contribution of the scattering is dominant for strongly dipole-allowed electronic transitions, HT effects are expected to play a major role for dipole-forbidden or weakly dipole-allowed transitions.

Porphyrin-related systems form an important class of compounds, which find applications, e.g., in photodynamic therapy, photocatalysis, or molecular electronics. Information on the excited states and about the photophysics of these compounds can be obtained using absorption and RR spectroscopy. Therefore, the interpretation of experimental data can strongly benefit from accurate calculations of the RR properties, helping in identifying the origin of the observed spectroscopic patterns. In particular, the absorption and RR spectra of porphyrin-based compounds are known to be significantly influenced by HT effects. For example, Minaev *et al.*[26] and Santoro *et al.*[27] have calculated the absorption spectrum of the S_1 state of free-base porphyrin and have found that HT effects largely dominate, while the FC contribution is significantly weaker due to the small transition dipole moment of the S_1 state. Additionally, Ma *et al.*[22] have reported calculated RR spectra of free-base porphyrin. Similar to absorption, they found that the RR intensities—assuming resonance with the S_1 state—almost entirely originate from the HT contribution. Moreover, Yang *et al.*[25] investigated theoretically the absorption spectra of three porphyrin-based compounds including two metalloporphyrins and an important constitutional isomer of porphyrin, i.e., *trans*-porphycene[28] (Fig. 1). For this latter compound, they found that the absorption spectrum of the S_1 state consists of a superposition of FC and HT contributions. Despite the fact that the properties of *trans*-porphycene have been extensively studied experimentally (see, e.g., Refs. 29 and 30)—especially using absorption or fluorescence spectroscopy[31,32] as well as RR or surface-enhanced RR scattering[33]—the RR properties of this compound were not yet investigated by theoretical calculations. Therefore, it

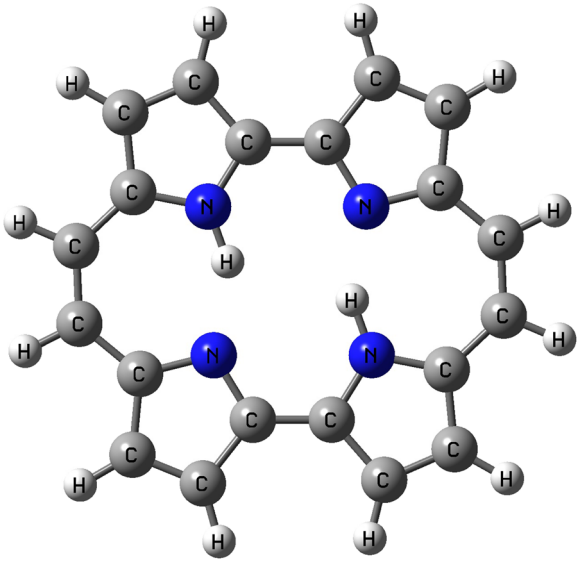

FIG. 1. Structure of the *trans*-porphycene molecule.

is the aim of this work to give a detailed study of the absorption and RR spectra and to analyze the role of HT effects. In particular, *trans*-porphycene is an excellent system to investigate a situation in which both FC and HT contributions have a comparable magnitude. Additionally, this study provides an assessment of the computational methods to simulate RR spectra.

The paper is organized as follows: Sec. II presents the main theory, approximations, and computational methods used to calculate the absorption and RR spectra. Section III A describes the excited state properties of the S_1 and S_2 states. Section III B reports and discusses the simulation of the absorption spectrum for the S_1 state. Section III C provides an analysis of the RR intensities. Finally, conclusions are given in Sec. IV.

II. THEORETICAL AND COMPUTATIONAL METHODS

The theory and methods employed to calculate the absorption and RR spectra were reported in details in a previous publication.[17] Therefore, only the main expressions and approximations are summarized in this section.

A. Calculation of resonance Raman cross sections

The differential (for the commonly employed 90° scattering geometry) Raman cross section for a transition between the initial $|i\rangle$ and final $|f\rangle$ vibronic states is given by[1,2]

$$\frac{d\sigma_{i\to f}}{d\Omega} = \frac{\omega_L \omega_S^3}{16\pi^2 \varepsilon_0^2 c^4} \frac{1}{45}(45a^2 + 5\delta^2 + 7\gamma^2), \qquad (1)$$

where ω_L is the frequency of the incident light, ω_S is the frequency of the scattered light, and a^2, δ^2, and γ^2 are the three Raman invariants for randomly oriented molecules, which depend on the Raman polarizability tensor $(\alpha_{\rho\sigma})_{i\to f}$.

The following approximations are introduced (see Ref. 17):

(i) The excitation frequency ω_L is in close resonance with a single electronic excited state (e) and only the "resonant" term in $(\alpha_{\rho\sigma})_{i\to f}$ is kept.
(ii) The Born-Oppenheimer and harmonic oscillator approximations are employed.
(iii) The electronic transition dipole moment is expanded in a Taylor series at the ground state geometry. The expansion is truncated after the linear term.

Under approximations (i)-(iii), the RR polarizability tensor for a fundamental transition from the electronic and vibrational ground state $|g0\rangle$ to the vibronic state $|g1_n\rangle$ can be written in the form

$$\left(\alpha_{\rho\sigma}\right)_{g0\to g1_n} = \frac{1}{\hbar\sqrt{2}} \left\{(FC)_e^{RR} + (FC/HT)_e^{RR} + (HT)_e^{RR}\right\}, \qquad (2)$$

where $(FC)_e^{RR}$, $(FC/HT)_e^{RR}$, and $(HT)_e^{RR}$ are the FC, the FC/HT, and the HT contributions of the excited state (e) to the RR polarizability tensor, respectively. The FC contribution involves a product between the components of the transition dipole moment μ_ρ evaluated at the ground state geometry, the FC/HT contribution involves products between μ_ρ and its derivatives $(\mu_\rho)'_l$ with respect to the normal coordinates q_l, and the HT contribution involves products of the type $(\mu_\rho)'_l(\mu_\rho)'_{l'}$ (see Ref. 17).

This formulation requires the calculation of FC overlap integrals between the ground state (g) and the excited state (e) in the harmonic approximation. In the general case, in which the ground and excited states have different equilibrium geometries, different vibrational frequencies, and different normal coordinates (i.e., inclusion of Duschinsky rotation effects), the FC overlap integrals can be computed using recursive relations.[34] This approach was applied to both absorption and RR spectra including or neglecting HT effects (see, e.g., Refs. 35, 27, and 16). However, the simplest approximation to describe the potential energy surfaces (PESs) of the ground and excited states is to assume that both PESs share the same normal coordinates (neglecting Duschinsky rotation) and the same vibrational frequencies. This model is known as the independent mode displaced harmonic oscillator (IMDHO) model and, for several molecular systems, it was shown to provide a sufficiently accurate reproduction of the RR intensities (see, e.g., Refs. 36, 10, and 12). In this case, the difference between the ground and excited state PESs is only determined by the dimensionless displacements Δ_l along the normal coordinates (l). Within the IMDHO model, the required FC overlap integrals can be computed efficiently using simple recursive relations.[37] Thus, the FC and FC/HT contributions can be written as

$$(FC)_e^{RR} = \mu_\rho \mu_\sigma \Delta_n \{\Phi_e(\omega_L) - \Phi_e(\omega_L - \omega_n)\}, \qquad (3.1)$$

$$\begin{aligned}(FC/HT)_e^{RR} = {} & \mu_\rho (\mu_\sigma)'_n \Phi_e(\omega_L - \omega_n) + \left(\mu_\rho\right)'_n \mu_\sigma \Phi_e(\omega_L) \\ & + \sum_l \left\{\mu_\rho (\mu_\sigma)'_l + \left(\mu_\rho\right)'_l \mu_\sigma\right\} \frac{\Delta_n \Delta_l}{2} \\ & \times \{\Phi_e(\omega_L) - \Phi_e(\omega_L - \omega_n) - \Phi_e(\omega_L - \omega_l) \\ & + \Phi_e(\omega_L - \omega_n - \omega_l)\}, \end{aligned} \qquad (3.2)$$

and the expression for the HT contribution is given in Ref. 17. ω_l is the vibrational frequency of mode (l) and the function $\Phi_e(\omega_L)$ is defined as[36,38]

$$\Phi_e(\omega_L) \equiv \sum_v \frac{\langle\theta_{g0}|\theta_{ev}\rangle^2}{\omega_{eg} + \omega_{v0} - \omega_L - i\Gamma}, \tag{4}$$

where the summation is taken over all the vibrational states of the electronic excited state (e), $\langle\theta_{g0}|\theta_{ev}\rangle^2$ is a FC factor, and ω_{eg} and ω_{v0} describe the electronic and vibrational transition frequencies, respectively. The damping factor Γ describes a homogeneous broadening.

Within the so-called simplified Φ_e function approach,[17] the function Φ_e is approximated by

$$\Phi_e(\omega_L) \cong \frac{1}{\Omega_{eg} - \omega_L - i\Gamma}, \tag{5}$$

where Ω_{eg} is the vertical transition frequency.

Within the IMDHO model, the displacements can be calculated from the excited state energy gradients evaluated at the ground state geometry according to

$$\Delta_l = -\frac{1}{\omega_l}\left(\frac{\partial\Omega_{eg}}{\partial q_l}\right)_0. \tag{6}$$

The importance of HT effects can also be quantified by the depolarization ratio. For an incident linear polarized radiation in the commonly employed 90° scattering geometry, the depolarization ratio is obtained from the Raman invariants by[1]

$$\rho_l = \frac{3\gamma^2 + 5\delta^2}{45a^2 + 4\gamma^2}. \tag{7}$$

B. Calculation of absorption cross sections

The absorption cross section for transitions from an initial state $|i\rangle$ to an ensemble of final states $|f\rangle$ is given by

$$\sigma_A(\omega_L) = \frac{4\pi^2}{3c\hbar}\omega_L \sum_f \sum_{\rho=\{x,y,z\}} \left|\left\langle i\left|\mu_\rho\right|f\right\rangle\right|^2 \frac{\Gamma}{\pi} \frac{1}{\left(\omega_{fi} - \omega_L\right)^2 + \Gamma^2}. \tag{8}$$

In Eq. (8), ω_L is the frequency of the incident light, $\langle i|\mu_\rho|f\rangle$ is a component of the transition dipole moment, and $\omega_{fi} \equiv \left(E_f - E_i\right)/\hbar$ is the Bohr frequency between the initial (i) and final (f) states. A homogeneous broadening is described by a Lorentzian function with a damping factor Γ.

Using the approximations (ii) and (iii) of Sec. II A, the absorption cross section for a single electronic excited state can be written as the sum of the FC, FC/HT, and HT contributions,

$$\sigma_A(\omega_L) = \frac{4\pi}{3c\hbar}\omega_L \left\{(FC)_e^A + (FC/HT)_e^A + (HT)_e^A\right\}. \tag{9}$$

The explicit expressions for $(FC)_e^A$, $(FC/HT)_e^A$, and $(HT)_e^A$ are provided in Ref. 17.

C. Computational methods

Quantum chemical calculations were performed with the GAUSSIAN 09 program,[39] which provides the structural and electronic data necessary for the simulation of the absorption and RR spectra of *trans*-porphycene. All the calculations were performed in a vacuum by means of density functional theory (DFT) and time dependent DFT (TDDFT) using the B3LYP exchange-correlation functional with the 6-311G(d,p) basis set. The C_{2h} symmetry of *trans*-porphycene was maintained in these calculations. The geometry, harmonic vibrational frequencies, and normal coordinates of the ground state S_0 were obtained by DFT, whereas the vertical excitation energies and transition dipole moments of the S_1 and S_2 excited states were obtained by TDDFT. The geometries and harmonic vibrations of the excited states were also computed with TDDFT in order to estimate the adiabatic energies and to investigate Duschinsky rotation effects. The calculated frequencies were positive, confirming that the obtained structures for the S_0, S_1, and S_2 states correspond to minima of the PESs. To correct for the lack of anharmonicity and the approximate treatment of electron correlation, the harmonic frequencies were scaled by the factor 0.97.

A program developed locally is employed to calculate the RR cross sections and absorption spectra. In particular, this demands the computation of the geometrical displacements Δ_l, derivatives of the transition dipole moment $(\mu_\rho)'_l$, and FC overlap integrals $\langle\theta_{g0}|\theta_{ev}\rangle$. Within the IMDHO model, the displacements were calculated from the gradients [Eq. (6)] as well as by projecting the difference between the S_1 and S_0 geometries on the ground state normal coordinates. The latter displacements were also employed to compute absorption and RR spectra in association with Duschinsky effects. The FC overlap integrals were computed from the displacements, vibrational frequencies, and normal coordinates using recursive relations.[34] In each case, a nearly complete convergence of the FC factor summation was obtained, with a value of $\sum_v \langle\theta_{g0}|\theta_{ev}\rangle^2 > 0.99$. The derivatives $(\partial\Omega_{eg}/\partial q_l)_0$ and $(\mu_\rho)'_l$ were obtained by a two-point numerical differentiation procedure from the vertical excitation energies and transition dipole moments, which were computed with TDDFT for distorted structures resulting from the addition or subtraction of a finite displacement along the normal coordinates to the ground state geometry. The accuracy of the numerical derivatives was evaluated with a Romberg procedure and by comparing numerical and analytical energy derivatives. The errors arising from the finite differentiation are estimated to be less than 1%. In the simulation of the absorption and RR spectra, a value of Γ equal to 20 cm^{-1} was assumed to reproduce the experimental broadening of the absorption spectrum.[31] The transition frequency (i.e., ω_{eg} in the IMDHO model and Ω_{eg} using the simplified Φ_e method) was set to the value of 16 012 cm^{-1}, which corresponds to the experimental origin transition in the nitrogen matrix.[31] The RR spectra were simulated for an excitation frequency ω_L of 16 012 cm^{-1} in exact resonance with the origin transition and maximum of absorption. Finally, a Lorentzian function with a full width at half maximum (FWHM) of 5 cm^{-1} was employed to broaden the Raman intensities.

III. RESULTS

A. Excited states

It is known from experimental data[31,40] that, contrary to porphyrin, the two first singlet excited states, S_1 and S_2, of *trans*-porphycene lie close in energy. Therefore, before investigating the absorption and RR properties of the S_1 state, the calculated energy positions of the S_1 and S_2 states are discussed. The calculated vertical energies, the adiabatic energies, and the adiabatic energies including the zero-point vibrational energy (ZPVE) correction are given in Table I, whereas the associated orbitals and the excited state properties obtained with different basis sets are reported in the supplementary material (see Fig. S1 and Table S1). Increasing the basis set size from a 6-311G(d,p) basis set to a 6-311++G(2df,pd) basis set has a negligible impact on the excited state properties. For example, the vertical excitation energies are decreased by at the most 0.01 eV. Therefore, the 6-311G(d,p) basis set was employed in the further calculations. In the case of the S_1 state, a decrease of 0.14 eV is obtained between the vertical energy and the adiabatic energy including the ZPVE correction, whereas a smaller decrease of 0.06 eV is predicted for the S_2 state (see Table I). This difference can be associated with the larger geometrical variations calculated between the S_0 geometry and the S_1 geometry, compared to the variations obtained between the S_0 and S_2 geometries (see Fig. S2 of the supplementary material). The comparison with the experimental adiabatic values measured in the nitrogen matrix[31] shows that the theoretical adiabatic energies including the ZPVE correction are overestimated by 0.11 eV and 0.20 eV for the S_1 and S_2 states, respectively. This is a typical accuracy for TDDFT energy calculations (see, e.g., Ref. 41), which is in accordance with the previously reported theoretical vertical energies of *trans*-porphycene.[25] The comparison with experimental data recorded in the xenon matrix[31] or in the 2-methyltetrahydrofuran solvent[40] presents a similar agreement. Hence, even if slightly overestimated, the predicted energy separations of 0.11 eV and 0.19 eV between the S_1 and S_2 states using vertical and adiabatic energies, respectively, are in agreement with the experimental energy gap of about 0.1 eV. Moreover, the calculated oscillator strengths of 0.128 and 0.196 for the S_1 and S_2 states, respectively, are in good agreement with the experimental values of 0.12 and 0.16 measured in the 2-methyltetrahydrofuran solvent.[40] Additionally, due to the C_{2h} symmetry of *trans*-porphycene, the electronic transition dipole moments of the S_1 and S_2 states lie in the molecular plane (see Fig. S3 of the supplementary material). Similar to porphyrin, in which the transition dipole moments are orthogonal due to the D_{2h} symmetry,[31] the transition dipole moments of *trans*-porphycene are known to be nearly orthogonal.[42,43] Indeed, the transition dipole moment of the S_1 state is oriented along the NH–HN direction, whereas the transition dipole moment of S_2 is perpendicular to that direction. In the present calculations, an angle of 90.09° is obtained between both transition dipole moments. In particular, these results indicate that the direction and the norm of the S_1 state electronic transition dipole moment are accurately predicted by the theory. This quantity is important in the determination of the FC and FC/HT contributions of the absorption and RR spectra, whereas its derivatives enter the FC/HT and HT contributions.

TABLE I. Excited state excitation energies (eV) and oscillator strengths of *trans*-porphycene.[a]

State	Vertical (eV)	Adiabatic (eV)	Adiabatic + ZPVE correction (eV)	f	Expt. (eV)
S_1	2.24	2.19	2.10	0.128	1.99[b], 1.96[c], 1.96[d]
S_2	2.35	2.33	2.29	0.196	2.09[b], 2.07[c], 2.07[d]

[a]Calculations performed in a vacuum [TDDFT/B3LYP/6-311G(d,p)].
[b]Measured in the nitrogen matrix at 15K.[31]
[c]Measured in the xenon matrix at 15K.[31]
[d]Measured in the 2-methyltetrahydrofuran solvent.[40]

B. Absorption spectrum for the $S_0 \rightarrow S_1$ transition

In this section, the absorption spectrum for the first singlet excited state (S_1) is simulated. As mentioned in Sec. II C, a value of Γ equal to 20 cm^{-1} was employed to reproduce the experimental broadening, and the adiabatic transition frequency (ω_{eg}) was set to the value of 16 012 cm^{-1}, which corresponds to the experimental origin transition in the nitrogen matrix.[31] This is performed to facilitate the comparison with experimental data. The vibronic structure of the absorption spectrum was simulated according to Eq. (9). The results obtained in the FC approximation are presented at the top of Fig. 2 and made use of three different methods. Within the IMDHO model, the displacements were calculated from the energy gradients [Eq. (6)] as well as from the difference between the S_1 and S_0 geometries. Additionally, the spectrum including Duschinsky effects was simulated. The top of Fig. 2 shows that, for all the methods, the spectrum is dominated by the origin transition. Indeed, the calculated FC factors of the origin transition have values of 0.618, 0.582, and 0.573 using the energy gradients, the difference between the S_1 and S_0 geometries, and by including Duschinsky effects, respectively. This indicates that the changes in geometry between the S_0 and S_1 states (i.e., displacements) remain rather moderate. Nevertheless, a complicated vibronic structure, showing several overlapping bands, is obtained from the origin transition to about 18 000 cm^{-1}. As can be seen in the top inset of Fig. 2, the three methods provide rather similar results in the 16 000-16 500 cm^{-1} region, whereas larger differences are obtained between 16 500 and 18 000 cm^{-1}. The main difference in the 16 000-16 500 cm^{-1} region concerns a decrease of the intensities when using displacements obtained from the difference between the S_1 and S_0 geometries in comparison to displacements obtained from the energy gradients. However, in the 16 500-18 000 cm^{-1} region, this trend is reversed and, additionally, the Duschinsky effects are stronger. In particular, more intense bands are found near 17 000 cm^{-1}.

The bottom of Fig. 2 presents the absorption spectra calculated within the IMDHO model using energy gradients for the displacements. It is seen that the inclusion of the FC/HT contribution has a small effect on the spectrum. This can be related to the fact that the non-zero derivatives of the transition dipole moment $\vec{\mu}'_l$ are nearly orthogonal to the transition dipole moment $\vec{\mu}$ (see the Cartesian

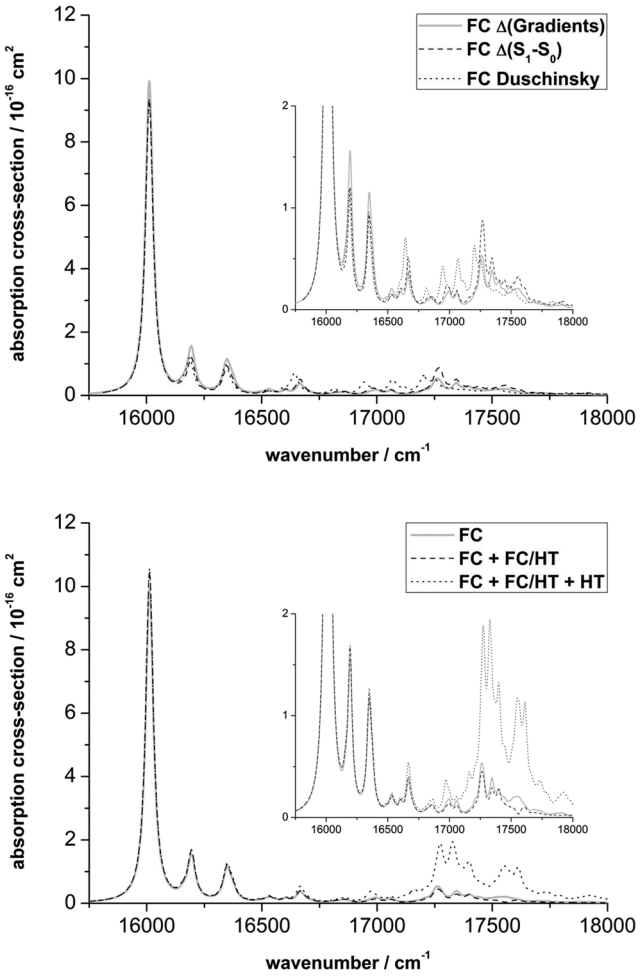

FIG. 2. Top: Comparison between absorption spectra calculated in the FC approximation. Δ's obtained from the gradients within the IMDHO model (gray line), Δ's obtained from the difference between the S_1 and S_0 geometries within the IMDHO model (dashed line), and including Duschinsky rotation effects (dotted line). Bottom: Absorption spectra calculated within the IMDHO model with Δ's obtained from the gradients. In the FC approximation (gray line), including FC and FC/HT terms (dashed line), and including FC, FC/HT, and HT terms (dotted line). The insets show a zoom on the low intensity bands.

components in Table S2 of the supplementary material). Because the FC/HT term involves the scalar products $\vec{\mu}'_l.\vec{\mu}$ (see Ref. 17), the effect of this contribution remains small. However, the HT contribution leads to a strong enhancement of the intensities between 17 000 and 18 000 cm^{-1}. This enhancement is directly related to the large $\vec{\mu}'_l$ values of the modes with vibrational frequencies between 900 and 1600 cm^{-1} (see Table S2 of the supplementary material). Indeed, the HT term depends on the scalar products $\vec{\mu}'_l.\vec{\mu}'_{l'}$ between the transition dipole moment derivatives (see Ref. 17). Comparing the top and bottom of Fig. 2 clearly shows that the HT effects have a much stronger impact on the absorption spectrum than Duschinsky effects and effects of different methods to calculate the displacements. This provides a justification of the use of the IMDHO model to investigate HT effects.

Figure 3 provides a comparison between the calculated spectrum of the S_1 state and the experimental spectrum recorded in the nitrogen matrix. The theoretical spectrum is obtained within the IMDHO model using displacements

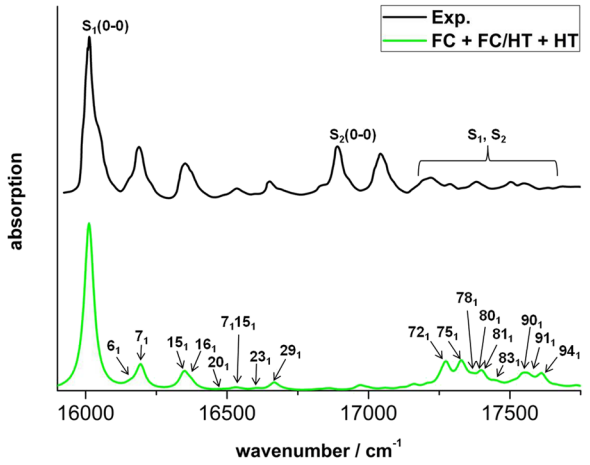

FIG. 3. Comparison between the calculated absorption spectrum including HT effects (green line) and the experimental spectrum[31] (black line) measured in the nitrogen matrix at 15K. The origin transitions (0-0) of the S_1 and S_2 states are indicated for the experimental spectrum. The main vibronic transitions are given for the calculated spectrum of the S_1 state.

calculated from the energy gradients and including FC, FC/HT, and HT contributions, while the experimental spectrum reported in Ref. 31 was digitized and plotted on Fig. 3. The measured spectrum consists of an overlap of the S_1 and S_2 states with origin transitions at 16 012 cm^{-1} and 16 894 cm^{-1}, respectively. The calculated spectrum is in good agreement with the experimental spectrum in the 16 000-16 750 cm^{-1} region. Indeed, the experimental vibronic structure is well reproduced and according to the calculations it originates mainly from the seven totally symmetric modes υ_6, υ_7, υ_{15}, υ_{16}, υ_{20}, υ_{23}, and υ_{29} (see modes in Table S3 of the supplementary material). In particular, the measured frequencies at 141, 178, 341, 362, 478, 592, and 638 cm^{-1} can be assigned to the seven associated fundamental transitions, whereas the measured frequency at 521 cm^{-1} is assigned to a combination of the modes υ_7 and υ_{15}. It can also be mentioned that all the methods, either including or not HT and Duschinsky effects, provide a good reproduction of the spectrum in this wavenumber range (see Fig. 2). Next, the experimental bands at 16 894 cm^{-1} and 17 049 cm^{-1} (i.e., 16 894 + 155 cm^{-1}) were assigned to the S_2 state[31] and are, therefore, not reproduced by the calculations. Nevertheless, the spectrum including Duschinsky effects (see Fig. 2) indicates that the S_1 bands near 17 000 cm^{-1} are enhanced. Similarly, the theoretical results reported by Yang *et al.*[25] for the S_1 state show that the inclusion of both Duschinsky and HT effects leads to an enhancement of the bands near 17 000 cm^{-1}. Therefore, these results suggest that some contributions of the S_1 state might overlap with the S_2 state to produce the experimental bands at 16 894 cm^{-1} and 17 049 cm^{-1}. Furthermore, the experimental bands in the 17 200-17 750 cm^{-1} region were assigned to a superposition of transitions to the S_1 or S_2 states.[31] In this respect, the calculations show that the S_1 contribution involves mainly nine fundamental transitions to the totally symmetric modes υ_{72}, υ_{75}, υ_{78}, υ_{80}, υ_{81}, υ_{83}, υ_{90}, υ_{91}, and υ_{94} (see modes in Table S3 of the supplementary material) and that these transitions are strongly enhanced due to HT effects (see Fig. 2).

C. Resonance Raman spectra

In this section, the RR spectra obtained for an excitation frequency ω_L of 16 012 cm^{-1}, in exact resonance with the S_1 state origin transition (i.e., maximum of absorption), are described. A value of Γ equal to 20 cm^{-1} was used to be consistent with the absorption data and a Lorentzian function with a FWHM of 5 cm^{-1} was employed to broaden the calculated Raman intensities.

The top of Fig. 4 considers the results calculated with the IMDHO model including the FC contribution and using displacements obtained either from the energy gradients or from the difference between the S_1 and S_0 geometries. Both methods provide comparable vibrational patterns. However, the RR intensities calculated from the energy gradients are larger in the 100–400 cm^{-1} range, whereas some modes (e.g., at 654.0 cm^{-1} and 1261.9 cm^{-1}) have larger RR intensities when using the displacements computed from the geometry difference. The bottom of Fig. 4 presents the spectra calculated in the FC approximation using displacements computed from the geometry difference within the IMDHO model and including Duschinsky effects. It is seen that the Duschinsky effects are very weak and that they mainly lead to a small decrease of the RR intensities in comparison to the IMDHO model. Therefore, the Duschinsky effect is almost negligible in the RR spectrum, whereas it produces changes in intensities and band positions in the absorption spectrum (see Fig. 2). This behavior can be explained from the fact that the Raman frequencies correspond to the ground state (S_0) vibrational modes (not the excited state modes) and from the fact that the excitation frequency ω_L is in resonance with the origin transition, for which Duschinsky effects in the absorption spectrum are small. Overall, these results indicate that the IMDHO model is adequate to reproduce the RR spectrum in resonance with the origin transition.

The top of Fig. 5 describes the effects of the FC/HT and HT contributions on the RR spectrum within the IMDHO model and using displacements computed from the energy gradients. As Fig. 5 shows, the HT effects lead to a strong enhancement of the RR intensities, in particular, for the vibrational modes above 1000 cm^{-1}. The enhancement due to HT effects is larger for the RR intensities than the one obtained for the

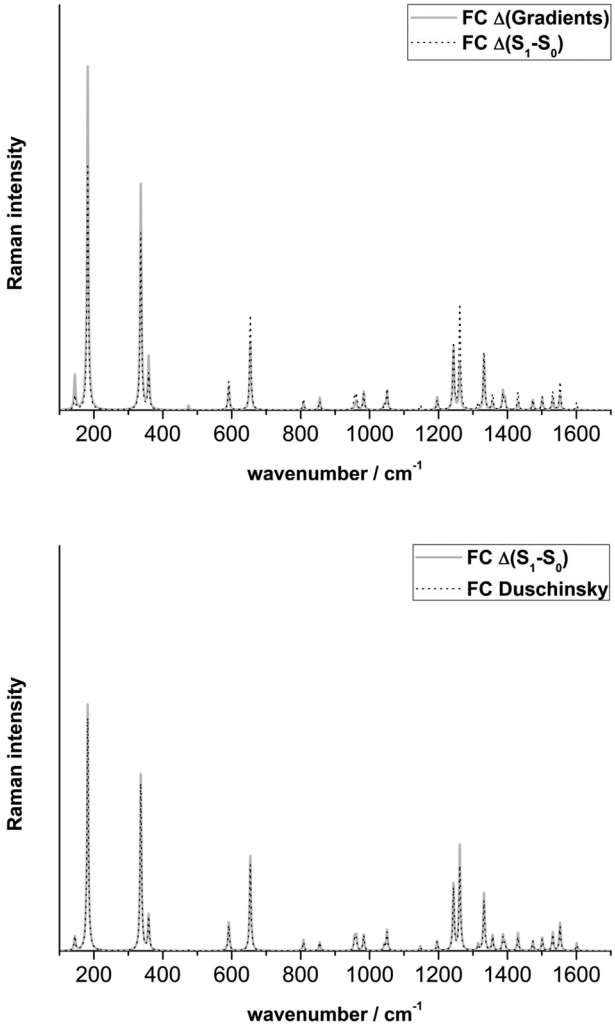

FIG. 4. Comparison between RR spectra calculated in the FC approximation. Δ's obtained from the gradients within the IMDHO model (top: gray line), Δ's obtained from the difference between the S_1 and S_0 geometries within the IMDHO model (top: dotted line, bottom: gray line), and including Duschinsky rotation effects (bottom: dotted line).

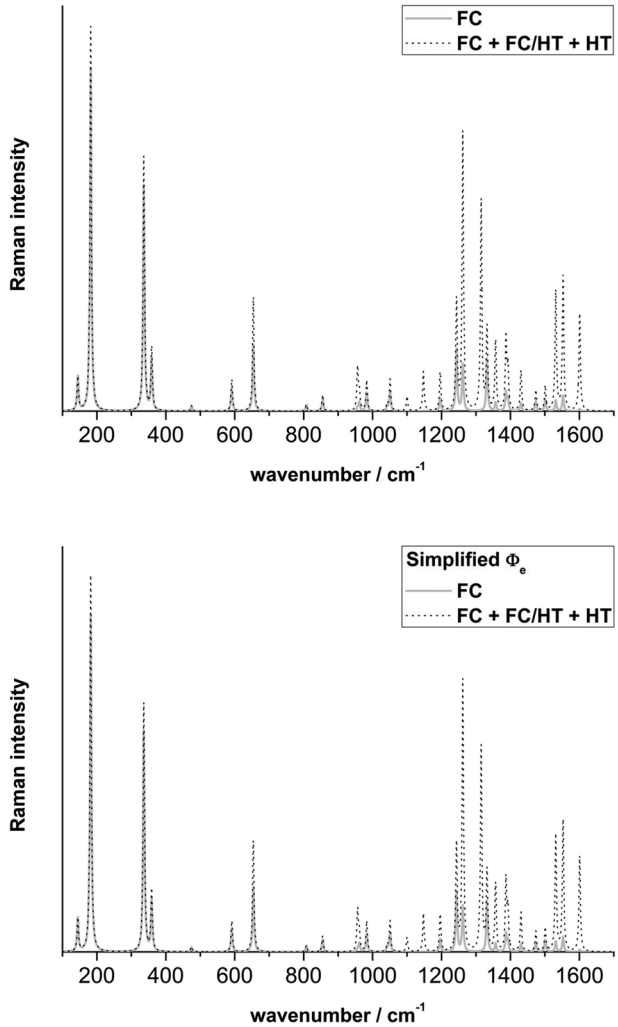

FIG. 5. Comparison between RR spectra calculated in the FC approximation (gray line) and including HT effects (dotted line) with Δ's obtained from the gradients. Top: IMDHO model. Bottom: Simplified Φ_e approximation.

absorption spectrum. Such a stronger sensitivity of RR intensities to HT effects was already noticed for others compounds (see, e.g., Refs. 17, 13, and 9). The investigation of the relative importance of the FC/HT and HT contributions (see Fig. S4 of the supplementary material) demonstrates that the HT effects almost entirely originate from the FC/HT contribution, while the higher-order HT contribution is nearly negligible in the present case. This is in contrast with the absorption spectrum, in which the HT contribution is mainly responsible of the HT effects. However, similar to absorption, the HT effects have a much stronger impact on the RR intensities than the Duschinsky effects and the effects of different methods to calculate the displacements.

The bottom of Fig. 5 presents the RR spectra obtained using the simplified Φ_e approximation. Comparison with the spectra on the top of Fig. 5 clearly shows that the simplified Φ_e method provides very similar results as the IMDHO model. This concerns both the FC and FC + FC/HT + HT approximations. In particular, the simplified Φ_e method perfectly reproduces the strong enhancement of the high frequency modes occurring from HT effects. Therefore, it is seen that neglecting the FC factors in the Φ_e function [Eq. (5)] has only a minor effect on the relative RR intensities and that this approximation is adequate to reproduce the RR spectrum including both FC and HT effects. It should be mentioned that the good performance of the simplified Φ_e method relies here on the facts that the absorption spectrum is dominated by the band at the origin (i.e., small values of displacements) and that the excitation frequency is in resonance with the origin transition (see Ref. 17).

Figure 6 provides a comparison between the calculated RR spectra and the experimental spectrum[33] that was recorded in polycrystalline thin films at an excitation wavelength of 632.8 nm (i.e., 15 803 cm^{-1}) in resonance with the S_1 state. The theoretical RR spectra are obtained within the IMDHO model employing displacements calculated from the energy gradients and using the FC and FC + FC/HT + HT approximations, while the experimental RR spectrum reported in Ref. 33 was digitized and plotted in Fig. 6. To allow an easier comparison of the relative RR intensities, all the spectra were normalized with respect to the more intense band, and a Lorentzian function with a FWHM of 20 cm^{-1} was employed to reproduce the experimental broadening. The vibrational frequencies, displacements, transition dipole moment derivatives, and RR differential cross sections are reported in Table II. As is clearly seen from Fig. 6, the inclusion of HT effects significantly improves the agreement with the experimental results. Indeed, the RR intensities in the 900–1650 cm^{-1} range are strongly underestimated when using the FC approximation, whereas the incorporation of the HT contributions leads to an enhancement of the bands, which is in better agreement with the experimental spectrum. The remaining discrepancies between the calculated and measured RR spectra can be ascribed to environmental effects—which are not taken into account in the present calculations—and to the intrinsic accuracy of the computational methods.

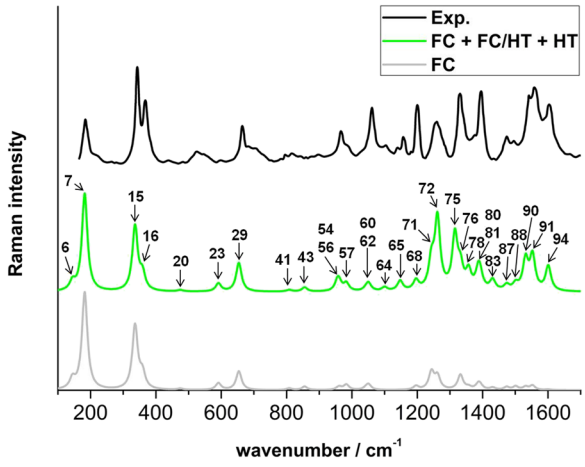

FIG. 6. Comparison between calculated RR spectra, in the FC approximation (gray line), including HT effects (green line), and the experimental spectrum[33] (black line) measured in polycrystalline thin film at an excitation wavelength of 632.8 nm. In the calculated spectra, a Lorentzian function with a FWHM of 20 cm^{-1} was employed to broaden the RR intensities. The thirty A_g modes associated with the fundamental transitions are indicated for the calculated spectrum.

The analysis of the data reveals that the calculated RR spectra result from 30 fundamental transitions (Fig. 6). These transitions are associated with the 30 lowest totally symmetric (A_g) modes of *trans*-porphycene in the 100–1650 cm^{-1} range (Table II and Table S3 of the supplementary material). Due to the C_{2h} symmetry of *trans*-porphycene, the vibrational modes with B_g symmetry could have a non-zero Raman intensity arising from the FC/HT contribution. However, the calculated transition dipole moment derivatives along these modes are very small (see Table S2 of the supplementary material), which leads to negligible RR intensities. The calculated vibrational frequencies of the A_g modes are compared to experimental Raman frequencies measured in nitrogen or xenon matrices[30] (Table II). A mean absolute deviation of 8.4 cm^{-1} is obtained between the theoretical harmonic frequencies (scaled by a factor of 0.97) and the experimental frequencies, which is a typical accuracy for B3LYP calculations.

From the comparison between the FC and the FC + FC/HT + HT approximations, it is seen that most of the RR active modes have an intensity arising both from the FC and FC/HT contributions, which indicates that an accurate prediction of the transition dipole moment (i.e., the calculated norm is 1.5280 a.u. for S_1) together with its derivatives (Table II, the largest value is obtained for mode υ_{75} at 0.0599 a.u.) is required to appropriately reproduce the relative RR intensities. Nevertheless, several modes also gain RR intensity almost exclusively from the HT effects (Table II). This is particularly the case for the modes υ_{54}, υ_{64}, υ_{65}, υ_{75}, and υ_{94}, which have small values of the displacements and large values of the transition dipole moment derivatives. Because these modes are observed in the experimental RR spectrum, it further highlights that the inclusion of HT effects is mandatory to properly describe the RR spectrum of *trans*-porphycene.

The HT effects can also be quantified through the determination of the depolarization ratios ρ_l [Eq. (7)]. Indeed, in the FC approximation, the depolarization ratios are exactly equal to 1/3, while the inclusion of HT effects leads to an increase of the values of ρ_l. On the one hand, the vibrational modes that are dominated by the FC contribution or

TABLE II. Vibrational frequencies (ν), displacements (Δ), norm of the transition dipole moment derivatives ($|\vec{\mu}'|$), and RR differential cross sections ($d\sigma/d\Omega$) of *trans*-porphycene.

	ν (cm^{-1})				$d\sigma/d\Omega$ (10^{-25} cm^2)	
Mode	Cal.[a]	Expt.[b]	Δ (dimensionless)	$\|\vec{\mu}'\|$ (a.u.)	FC	FC + FC/HT + HT[c]
6	144.6	150	0.166	0.0014	19.9	19.6 (0.36)
7	182.0	182	0.527	0.0003	200.0	223.8 (0.33)
15	336.2	342	−0.432	0.0020	131.5	147.9 (0.34)
16	358.9	367	0.208	0.0040	30.3	36.3 (0.38)
20	474.5	482	0.063	0.0009	2.7	3.2 (0.36)
23	591.4	591	−0.144	0.0017	14.0	18.4 (0.34)
29	654.0	667	−0.241	0.0151	38.7	66.3 (0.56)
41	808.1	811	−0.076	0.0009	3.7	3.9 (0.34)
43	855.2	859	0.107	0.0047	7.4	9.5 (0.44)
54	956.5	966	−0.054	0.0198	1.8	24.4 (1.35)
56	961.6	972	0.091	0.0089	5.2	10.6 (0.68)
57	983.0	993	0.132	0.0027	10.9	17.7 (0.33)
60	1042.6	1054	−0.070	0.0014	3.0	4.0 (0.35)
62	1050.7	1062	0.136	0.0039	11.3	18.4 (0.35)
64	1100.1	1116	−0.007	0.0143	<0.1	8.6 (1.99)
65	1147.7	1159	−0.015	0.0236	1.4	22.9 (1.84)
68	1196.3	1200	−0.113	0.0179	7.6	22.1 (0.91)
71	1243.6	1251	−0.246	0.0147	36.0	63.5 (0.42)
72	1261.9	1264	0.214	0.0567	27.2	161.6 (1.17)
75	1315.2	1331*	0.009	0.0599	0.1	122.1 (1.87)
76	1332.2	1342	0.229	0.0047	30.5	47.3 (0.33)
78	1357.1	1375	−0.092	0.0308	4.9	40.3 (1.27)
80	1387.1	1398	0.137	0.0349	10.8	41.9 (1.62)
81	1392.8	1408	−0.105	0.0230	6.4	23.5 (1.19)
83	1430.7	1428	0.091	0.0193	4.7	23.3 (0.75)
87	1473.9	1471*	0.102	0.0087	6.0	12.0 (0.46)
88	1501.1	1494*	0.112	0.0052	7.1	14.2 (0.34)
90	1531.6	1542	0.106	0.0421	6.3	69.6 (1.07)
91	1552.9	1563	0.128	0.0415	9.1	78.0 (0.87)
94	1601.1	1609	−0.048	0.0460	1.3	56.6 (1.90)

[a]Calculated harmonic frequencies scaled by a factor of 0.97.
[b]Raman vibrational frequencies[30] measured in nitrogen or xenon (indicated by *) matrices at 10K.
[c]Depolarization ratio values are given in brackets.

that show a small HT enhancement have a depolarization ratio close to 0.33 (Table II). This is particularly visible for the frequency modes below 600 cm^{-1} and for several higher frequency modes having small transition dipole moment derivatives. On the other hand, the vibrational modes with larger values of the transition dipole moment derivatives have much larger depolarization ratios with values nearly as large as 2.00 for the modes having negligible FC intensity, e.g., modes υ_{64}, υ_{65}, υ_{75}, and υ_{94} (see the supplementary material for an explanation of the boundary values of ρ_l). Therefore, the HT effects occurring in *trans*-porphycene could in principle be observed through the measurements of the depolarization ratios.

IV. CONCLUSIONS

The geometries, the vibrational frequencies, the excited state properties, the vibronic structure in the absorption spectrum of the S_1 state, and the RR intensities in resonance with the S_1 state have been investigated for *trans*-porphycene using different theoretical methods. A particular emphasis has been put in the evaluation of the HT effects and on their role in the absorption and RR spectra. An assessment of the theoretical results was also performed through a comparison with experimental data. It was found that (i) the energy separation between the S_1 and S_2 states as well as the norm and direction of the S_1 transition dipole moment are accurately predicted by the theory, (ii) the changes in geometry between the S_0 and S_1 states (i.e., displacements) remain rather moderate, which leads to a strong intensity of the origin transition in the absorption spectrum, (iii) the HT effects are stronger for the RR intensities than for the absorption intensities, (iv) the HT enhancement originates from the FC/HT contribution in the RR spectrum, whereas the HT effects are dominated by the pure HT contribution in the absorption spectrum, (v) the effects of Duschinsky rotation and of different methods to calculate the displacements have a much weaker impact on the absorption and RR spectra than HT effects, (vi) Duschinsky effects lead to noticeable modifications in the absorption intensities but are nearly negligible in the RR spectrum, which provides a validation of the IMDHO model, (vii) the simplified Φ_e approximation gives an excellent reproduction of the RR spectra obtained

with the IMDHO model, (viii) the simulated absorption spectrum is in good agreement with the experimental results in the 16 000-16 750 cm^{-1} region, and the inclusion of HT effects significantly improves the agreement between the calculated and experimental RR spectra, and (ix) the HT effects occurring in the RR intensities of *trans*-porphycene lead to different values of the depolarization ratio, which can be used to quantify the relative importance of the FC and FC/HT contributions. The values of ρ_I can be in principle obtained from experiment, which provides an opportunity to measure the magnitude of HT effects. Generally, it can be concluded that HT effects have a significant role on the RR spectrum of *trans*-porphycene and that their inclusion in the computational scheme is mandatory to accurately predict the RR intensities. Finally, comparable effects are to be expected for related porphycene-based compounds, in which structural modifications can be employed to tune the relative magnitude of the FC and FC/HT contributions.

SUPPLEMENTARY MATERIAL

See supplementary material for additional details about the geometries, vibrational modes, excited states properties, orbitals, RR intensities, and depolarization ratio.

ACKNOWLEDGMENTS

The author is thankful to Professor Jacek Waluk for interesting discussions regarding the properties of porphycenes. This work is supported by the Narodowe Centrum Nauki (NCN) (Project No. 2014/14/M/ST4/00083). The calculations have been performed at the Universitätsrechenzentrum of the Friedrich-Schiller University of Jena and at the Wrocław Centre for Networking and Supercomputing (Grant No. 384).

[1] D. A. Long, *The Raman Effect: A Unified Treatment of the Theory of Raman Scattering by Molecules* (John Wiley & Sons Ltd., New York, 2002).
[2] A. C. Albrecht, J. Chem. Phys. **34**, 1476 (1961).
[3] M. Wächtler, J. Guthmuller, L. González, and B. Dietzek, Coord. Chem. Rev. **256**, 1479 (2012).
[4] E. J. Heller, R. L. Sundberg, and D. Tannor, J. Phys. Chem. **86**, 1822 (1982).
[5] W. L. Peticolas and T. Rush, J. Comput. Chem. **16**, 1261 (1995).
[6] J. Guthmuller, J. Chem. Theory Comput. **7**, 1082 (2011).
[7] S. Kupfer, J. Guthmuller, and L. González, J. Chem. Theory Comput. **9**, 543 (2013).
[8] M. Staniszewska, S. Kupfer, M. Łabuda, and J. Guthmuller, J. Chem. Theory Comput. **13**, 1263 (2017).
[9] N. Lin, V. Barone, C. Cappelli, X. Zhao, K. Ruud, and F. Santoro, Mol. Phys. **111**, 1511 (2013).
[10] J. Guthmuller and B. Champagne, ChemPhysChem **9**, 1667 (2008).
[11] J. Romanova, V. Liégeois, and B. Champagne, Phys. Chem. Chem. Phys. **16**, 21721 (2014).
[12] S. Kupfer, M. Wächtler, J. Guthmuller, J. Popp, B. Dietzek, and L. González, J. Phys. Chem. C **116**, 19968 (2012).
[13] F. J. A. Ferrer, V. Barone, C. Cappelli, and F. Santoro, J. Chem. Theory Comput. **9**, 3597 (2013).
[14] J. Neugebauer and B. A. Hess, J. Chem. Phys. **120**, 11564 (2004).
[15] K. A. Kane and L. Jensen, J. Phys. Chem. C **114**, 5540 (2010).
[16] F. Santoro, C. Cappelli, and V. Barone, J. Chem. Theory Comput. **7**, 1824 (2011).
[17] J. Guthmuller, J. Chem. Phys. **144**, 064106 (2016).
[18] S.-Y. Lee and E. J. Heller, J. Chem. Phys. **71**, 4777 (1979).
[19] D. J. Tannor and E. J. Heller, J. Chem. Phys. **77**, 202 (1982).
[20] T. Petrenko and F. Neese, J. Chem. Phys. **137**, 234107 (2012).
[21] D. W. Silverstein and L. Jensen, J. Chem. Phys. **136**, 064111 (2012).
[22] H. Ma, J. Liu, and W. Liang, J. Chem. Theory Comput. **8**, 4474 (2012).
[23] A. Baiardi, J. Bloino, and V. Barone, J. Chem. Phys. **141**, 114108 (2014).
[24] F. Egidi, J. Bloino, C. Cappelli, and V. Barone, J. Chem. Theory Comput. **10**, 346 (2014).
[25] P. Yang, D. Qi, G. You, W. Shen, M. Li, and R. He, J. Chem. Phys. **141**, 124304 (2014).
[26] B. Minaev, Y.-H. Wang, C.-K. Wang, Y. Luo, and H. Ågren, Spectrochim. Acta, Part A **65**, 308 (2006).
[27] F. Santoro, A. Lami, R. Improta, J. Bloino, and V. Barone, J. Chem. Phys. **128**, 224311 (2008).
[28] E. Vogel, M. Köcher, H. Schmickler, and J. Lex, Angew. Chem., Int. Ed. **25**, 257 (1986).
[29] J. Waluk, Chem. Rev. **117**, 2447 (2017).
[30] S. Gawinkowski, Ł. Walewski, A. Vdovin, A. Slenczka, S. Rols, M. R. Johnson, B. Lesyng, and J. Waluk, Phys. Chem. Chem. Phys. **14**, 5489 (2012).
[31] A. Starukhin, E. Vogel, and J. Waluk, J. Phys. Chem. A **102**, 9999 (1998).
[32] E. T. Mengesha, J. Sepioł, P. Borowicz, and J. Waluk, J. Chem. Phys. **138**, 174201 (2013).
[33] S. Gawinkowski, M. Pszona, A. Gorski, J. Niedziółka-Jönsson, I. Kamińska, W. Nogala, and J. Waluk, Nanoscale **8**, 3337 (2016).
[34] P. T. Ruhoff, Chem. Phys. **186**, 355 (1994).
[35] J. Guthmuller, F. Zutterman, and B. Champagne, J. Chem. Phys. **131**, 154302 (2009).
[36] J. Guthmuller and B. Champagne, J. Chem. Phys. **127**, 164507 (2007).
[37] C. Manneback, Physica **17**, 1001 (1951).
[38] D. L. Tonks and J. B. Page, Chem. Phys. Lett. **66**, 449 (1979).
[39] M. J. Frisch, G. W. Trucks, H. B. Schlegel, G. E. Scuseria, M. A. Robb, J. R. Cheeseman, G. Scalmani, V. Barone, B. Mennucci, G. A. Petersson, H. Nakatsuji, M. Caricato, X. Li, H. P. Hratchian, A. F. Izmaylov, J. Bloino, G. Zheng, J. L. Sonnenberg, M. Hada, M. Ehara, K. Toyota, R. Fukuda, J. Hasegawa, M. Ishida, T. Nakajima, Y. Honda, O. Kitao, H. Nakai, T. Vreven, J. J. A. Montgomery, J. E. Peralta, F. Ogliaro, M. Bearpark, J. J. Heyd, E. Brothers, K. N. Kudin, V. N. Staroverov, R. Kobayashi, J. Normand, K. Raghavachari, A. Rendell, J. C. Burant, S. S. Iyengar, J. Tomasi, M. Cossi, N. Rega, J. M. Millam, M. Klene, J. E. Knox, J. B. Cross, V. Bakken, C. Adamo, J. Jaramillo, R. Gomperts, R. E. Stratmann, O. Yazyev, A. J. Austin, R. Cammi, C. Pomelli, J. W. Ochterski, R. L. Martin, K. Morokuma, V. G. Zakrzewski, G. A. Voth, P. Salvador, J. J. Dannenberg, S. Dapprich, A. D. Daniels, O. Farkas, J. B. Foresman, J. V. Ortiz, J. Cioslowski, and D. J. Fox, GAUSSIAN 09, Revision A.02, Gaussian, Inc., Wallingford, CT, 2009.
[40] J. Waluk, M. Müller, P. Swiderek, M. Köcher, E. Vogel, G. Hohlneicher, and J. Michl, J. Am. Chem. Soc. **113**, 5511 (1991).
[41] A. D. Laurent and D. Jacquemin, Int. J. Quantum Chem. **113**, 2019 (2013).
[42] J. Waluk and E. Vogel, J. Phys. Chem. **98**, 4530 (1994).
[43] K. Birklund-Andersen, E. Vogel, and J. Waluk, Chem. Phys. Lett. **271**, 341 (1997).